TÜBİTAK

Turkish Journal of Chemistry

http://journals.tubitak.gov.tr/chem/

Research Article

Turk J Chem
(2022) 46: 999-1010

doi:10.55730/1300-0527.3410

# $CO_2$ absorption into primary and secondary amine aqueous solutions with and without copper ions in a bubble column

**Hamed YOUSEFZADEH[1], Cansu GÜLER[2], Can ERKEY[1], Erdal UZUNLAR[2,*]**

[1]Department of Chemical and Biological Engineering, Koç University, İstanbul, Turkey
[2]Department of Chemical Engineering, İzmir Institute of Technology, İzmir, Turkey

**Received:** 31.08.2021 • **Accepted/Published Online:** 23.02.2022 • **Final Version:** 05.08.2022

**Abstract:** Chemical absorption of $CO_2$ into aqueous amine solutions using a nonstirred bubble column was experimentally investigated. The performance of $CO_2$ absorption of four different primary and secondary amines including monoethanolamine (MEA), piperazine (PZ), 2-piperidineethanol (2PE), and homopiperazine (HPZ) were compared. The effects of initial concentration of amine, the inlet mole fraction of $CO_2$, and solution temperature on the rate of $CO_2$ absorption and $CO_2$ loading (mol $CO_2$/mol amine) were studied in the range of 0.02–1 M, 0.10–0.15, and 25–40 °C, respectively. The effect of the presence of copper ions in the amine solution on $CO_2$ loading was also studied. By comparison of the breakthrough curves of the amines at different operational conditions, it was revealed that the shortest and longest time for the appearance of the breakthrough point was observed for MEA and HPZ solutions, respectively. $CO_2$ loading of MEA, 2PE, PZ, and HPZ aqueous solutions at 25 °C, 0.2 M of initial concentration of amine, and 0.15 of inlet mole fraction of $CO_2$ were 1.06, 1.14, 1.13, and 1.18 mol $CO_2$/mol amine, respectively. By decreasing the inlet mole fraction of $CO_2$ from 0.15 to 0.10, $CO_2$ loading slightly decreased. As the initial concentration of amine and temperature decreased, $CO_2$ loading increased. Also, the presence of copper ions in the absorbent solution resulted in a decrease in the $CO_2$ loading of MEA and HPZ aqueous solutions. In case of PZ and 2PE amines, adding copper ions led to precipitation even at low copper ion concentrations.

**Key words:** $CO_2$ absorption, carbon capture and storage, amine, copper, monoethanolamine, piperazine, homopiperazine, 2-piperidineethanol

## 1. Introduction

Global warming is the biggest environmental threat nowadays resulting in climate change with consequences such as rising sea levels, droughts, hurricanes, and extreme weather events [1]. Elevated concentration of greenhouse gasses ($CO_2$, $CH_4$, NOx) and especially of $CO_2$ in the atmosphere in recent decades, is the main reason for global warming [2]. Power plants are responsible for more than 40% of $CO_2$ emissions among which the coal-fired power plants release 73% of total $CO_2$ emissions of fossil fuel-based power plants [3, 4]. The utilization of fossil fuels, especially coal, will continue because fossil fuels are still the cheapest options to produce electricity. Thus, it will be desirable to remove $CO_2$ from the flue gas generated by power plants to stabilize the $CO_2$ levels in the atmosphere [5].

Adsorption [6], absorption [7], membrane separations [8], cryogenic distillation [9], and chemical looping [10] are the technologies being investigated for $CO_2$ capture from flue gas streams. Among these, post-combustion $CO_2$ absorption by amine scrubbing seems to be a viable method already implemented in some industrial units, due to the desired efficiency of $CO_2$ removal and ease of scale-up [11]. Also, amines are thermally regenerable solvents and have a strong affinity for $CO_2$. Thus, the technology consists of absorption of $CO_2$ by an aqueous amine solution at low temperature, generally, 40 °C, followed by regeneration of the amine solution at a higher temperature to release $CO_2$ and recycle the fresh amine solution back to the absorber column [12,13]. The type of $CO_2$ absorption using amines is chemical absorption during which dissolved $CO_2$ molecules react with the nucleophilic nitrogen atom of amines forming a chemical bond between the nitrogen of amine and carbon of $CO_2$. The physical and chemical properties of the $CO_2$-$H_2O$-amine system including viscosity, density, solubility of $CO_2$, reaction rate, mass transfer rate, and regeneration heat determine the solvent performance of $CO_2$ capture in the absorption/desorption system [11]. Amines are generally categorized into three main groups as primary, secondary, and tertiary amines [14]. Monoethanolamine (MEA) as a primary alkanolamine and piperazine (PZ) as a secondary amine have been frequently studied for $CO_2$-amine-water

* Correspondence: erdaluzunlar@iyte.edu.tr

systems in literature [15–21]. Especially, MEA aqueous solution is used as the absorbent in the industrial-scale $CO_2$ removing systems [5, 22].

Huge energy consumption for solvent regeneration is the main drawback of amine-based $CO_2$ capture systems. Electrochemical $CO_2$ capture technology, which is a relatively new method under development, stands out by directly eliminating the high energy consumption in the MEA process since it is a process carried out at a low temperature [23]. In addition, electrochemical $CO_2$ capture technology reduces electrical losses and prevents side reactions by precise control of potential. There are two main approaches to $CO_2$ capture by electrochemical methods in the literature: (i) using electrochemical processes for both $CO_2$ capture and $CO_2$ release (overall approach), (ii) conventional methods for $CO_2$ capture (e.g., MEA process) and $CO_2$ release using the electrochemical method (hybrid approach) [24]. In the hybrid approach, formed $CO_2$-amine complex is pumped to the anode of an electrochemical cell where metal ions (e.g., Cu(II)) are dissolved by the potential applied to the anode. These metal ions form a complex with the amine, allowing the amine-$CO_2$ complex to release $CO_2$. The resulting Cu(II)-amine complexes are pumped to the cathode in the electrochemical cell and the amine is liberated and recovered by reduction of the metal ion (reduced Cu(II) accumulates on the cathode as Cu(s)). Regenerated amine is then sent back to the absorption column. During the electrochemical regeneration, some copper-amine complexes stay in the aqueous phase [25] resulting in a decrease in $CO_2$ loading compared to the copper ions free amine solution due to occupying some portion of free amines by the formation of the metal-amine complexes [26]. Nevertheless, the presence of copper ions and the interaction between copper ions and amines enable the modulation of $CO_2$ loading in electrochemical $CO_2$ capture systems.

In this study, the rate of $CO_2$ absorption and $CO_2$ loading of four primary and secondary amines including monoethanolamine (MEA), piperazine (PZ), 2-piperdineethanol (2PE), and homopiperazine (HPZ) in a lab-scale bubble column were investigated. Effect of process parameters including temperature, $CO_2$ initial mole fraction, and amine concentration were studied by varying between 25–40 °C, 0.10–0.15, and 0.02–1 M, respectively. Also, the effect of the presence of copper ions in the amine solution on the $CO_2$ loading was also studied by varying the concentration of copper ions between 0.02–0.2 M and compared to absorption without any copper ions. This was carried out for amines such as PZ, HPZ, and 2PE for the first time in the literature.

## 2. Materials and methods

### 2.1. Materials

Monoethanolamine (hereafter referred to as MEA) was obtained from the TÜPRAŞ R&D center. Piperazine (PZ), homopiperazine (HPZ), 2-piperidineethanol (2PE), and copper (II) nitrate were purchased from Sigma-Aldrich. $CO_2$ and $N_2$ gases (99.999%) were obtained from Air Liquide. Ultra-pure water (MilliQ, 18.2 MΩ) was used to prepare amine solutions at the desired amine concentration as the absorbent.

### 2.2. Absorption setup

The schematic of the experimental setup of the $CO_2$ absorption system used in this study is shown in Figure 1. A graduated cylinder with an internal diameter of 3.2 cm and a total volume of 280 mL was used as the bubble column. The top of this cylinder was plugged using a stopper with three holes to insert the tubing for inlet flue gas, the outlet gas, and a thermometer. Teflon tubes were used for all the gas lines. Prior to sending the simulated flue gas into the bubble column, an aqueous solution containing a certain amount of amine and MilliQ water was prepared and placed in the bubble column. The temperature of the column and amine solution was tuned to the desired temperature using a water jacket connected to a heating water circulator (Cole Parmer, Model 12108-15). Also, the gas mixture line was preheated by a water jacket up to the amine solution temperature. The temperature of the solution during the absorption experiments was recorded using a thermometer. The flue gas mixture was simulated by combining $CO_2$ and $N_2$ gas delivered by calibrated mass flow controllers (MFC, Teledyne Hastings HFC202). The mole fraction of $CO_2$ in the gas mixture was adjusted by adjusting the volumetric flowrates of $CO_2$ and $N_2$ at 25 °C and atmospheric pressure. The flow rate of the gas mixture was kept constant at 250 mL/min. In the first stage, the entire inlet line was cleaned using a bypass line with pure nitrogen. Then, $N_2$ gas was passed through the bubble column and the outlet line between the column and the $CO_2$ sensor (GasLab, SprintIR®-W 100% $CO_2$ sensor) was cleaned in the same way until the sensor showed zero mole fraction of $CO_2$. Then, $CO_2$ was added to the gas stream at a certain $CO_2$ mole fraction and this time was recorded as the start time of $CO_2$ absorption. The inlet gas line was sent through the stopper hole to the bottom of the bubble column and bubbled through an air stone before mixing it into the amine solution. $CO_2$ in a gas mixture with a high concentration is captured by the amine solution in the column, and a gas mixture with zero or low $CO_2$ concentration is obtained in the outlet. The amine and water vapor were removed from the outlet gas mixture using a condenser at 5 °C to prevent damaging the $CO_2$ sensor by the amine and water vapor. Since the amount of amine vapor in the gas mixture leaving the condenser was negligible due to a very high Henry's constant and vapor pressure of water was low at 5 °C, it was

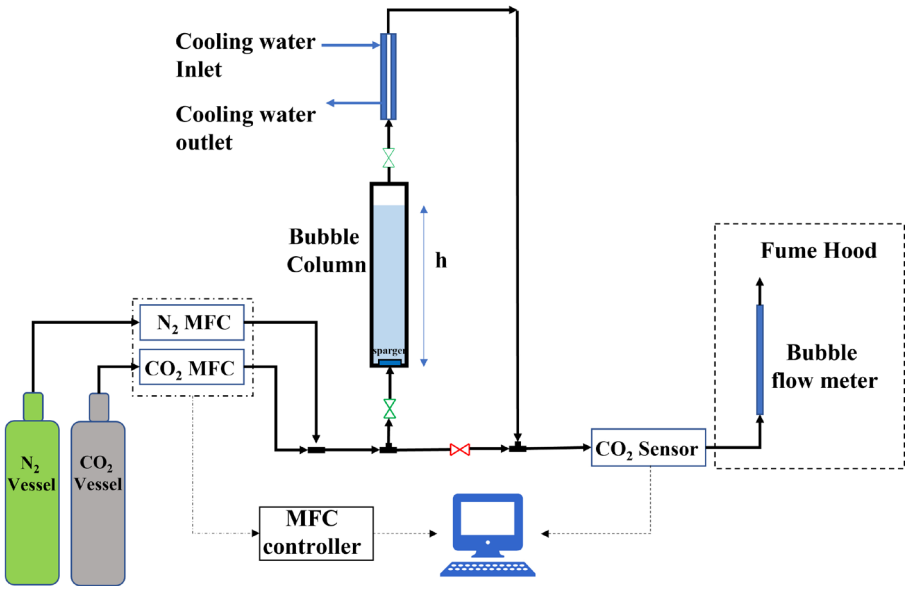


**Figure 1.** Experimental setup of $CO_2$ absorption into amine solutions using a bubble column.

assumed that the outlet gas mixture consisted of only $N_2$ and $CO_2$. The mole fraction of $CO_2$ in the outlet gas mixture was measured using the online $CO_2$ sensor until the mole fraction reached the inlet mole fraction of $CO_2$ (equilibrium condition). In every absorption experiment, the output $CO_2$ concentration was plotted against time. This curve is called the breakthrough curve. Typically, in a breakthrough curve, a zero-outlet concentration of the compound of interest is observed up to a certain time after which the outlet concentration starts to increase. The time at which the outlet concentration reaches 5% of inlet concentration is called the breakthrough time. Also, saturation time is the time at which the inlet and outlet concentrations become identical. After this time, the system is in a liquid-gas thermodynamic equilibrium state.

### 2.3. Measurement of the rate of $CO_2$ absorption

Mass balance for $CO_2$ in the gas phase was performed to determine the rate of $CO_2$ absorption from the gas phase into the liquid phase, as shown by equation (1).

$$F_{CO_2(g),in} - F_{CO_2(g),out} - r_{CO_2,(absorption)} = \frac{dN_{CO_2(g)}}{dt} \tag{1}$$

The accumulation term of equation (1) was rewritten in terms of the gas phase volume, concentration, and mole fraction of $CO_2$ in the outlet gas mixture assuming a well-mixed solution in the column as follows:

$$\frac{dN_{CO_2(g)}}{dt} = C_{out}.V_g.\frac{dy_{CO_2(g),out}}{dt} \tag{2}$$

Assuming an ideal gas mixture, the total concentration of the outlet gas mixture was calculated as follows:

$$C_{out} = \frac{P_{out}}{RT_{out}} \tag{3}$$

where $P_{out}$ was equal to 1 atm and $T_{out}$ was taken as absorption column temperature, respectively.

The molar flow rate of $CO_2$ in outlet, $P_{CO_2(g),out}$ was rewritten as follows:

$$F_{CO_2(g),out} = F_{N_2(g),out}\left(\frac{y_{CO_2(g),out}}{1-y_{CO_2(g),out}}\right) \tag{4}$$

The molar flow rate of nitrogen was assumed to be constant. Using equations (2), (3), and (4), the rate of absorption was derived from equation (1) as follows:

$$r_{absorption} = F_{CO_2(g),in} - F_{N_2,in}\left(\frac{y_{CO_2(g),out}}{1-y_{CO_2(g),out}}\right) - C_{out}.V_g.\frac{dy_{CO_2(g),out}}{dt} \tag{5}$$

The concentration of $CO_2$ in the outlet gas mixture was measured and recorded by the sensor every 5 s. For each time the absorption rate was calculated using equation (5). The absorption rate data was plotted against time for each experiment.

### 2.4. Measurement of $CO_2$ loading

The integral of the absorption rate versus time was equal to $CO_2$ loading of the corresponding amine solution as shown in equation (6). The $CO_2$ loading was calculated for all the experiments with different amines and process conditions. Effects of amine type (MEA, PZ, HPZ, 2PE), initial concentration of amine (0.02 M–1 M), inlet $CO_2$ gas mol fraction (0.1 and 0.15), and amine solution temperature (25–40 °C) on $CO_2$ loading were investigated.

$$\alpha_{CO_2} = \int_0^{t_{final}} \left[ F_{CO_2(g),in} - F_{N_2,in} \left( \frac{y_{CO_2(g),out}}{1 - y_{CO_2(g),out}} \right) - C_{out} . V_g . \frac{dy_{CO_2(g),out}}{dt} \right] dt \tag{6}$$

## 3. Results and discussion

### 3.1. Breakthrough curves and $CO_2$ loading

According to the breakthrough curves given in Figure 2, the mole fraction of $CO_2$ was zero at the outlet for a while, indicating that all the $CO_2$ of the inlet stream was absorbed by the solution. After the breakthrough point was reached in each curve, the mole fraction of $CO_2$ at the outlet stream started to increase more rapidly and finally reached the saturation point where the inlet and outlet mole fractions of $CO_2$ were equal. The breakthrough curves for $CO_2$ absorption of different amines at 25 °C shown in Figure 2a were obtained when the initial mole fraction of $CO_2$ and initial concentration of amine were 0.15 and 0.2 M, respectively. The breakthrough time was approximately 1000, 1230, 1520, and 1700 s for MEA, 2PE, PZ, and HPZ, respectively. The breakthrough was observed after 2850, 3000, 3250, and 4300 s for 2PE, HPZ, PZ, and MEA, respectively. MEA was the amine with the fastest breakthrough but the latest to the saturation point. The effect of the initial concentration of amines on the rate of $CO_2$ absorption and loading was investigated by lowering the initial concentration of amines from 0.2 M to 0.1 M while keeping other parameters unchanged. The breakthrough time and equilibrium state were obtained earlier at a low initial concentration of amines, as shown in Figure 2b. The breakthrough occurred at 500,

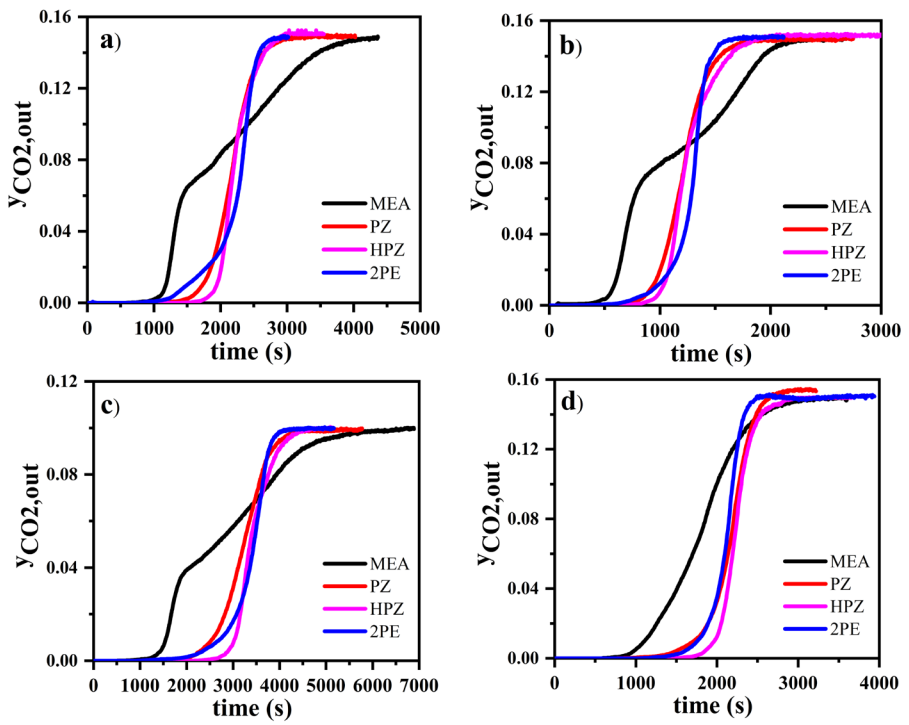


**Figure 2.** Breakthrough curves of $CO_2$ absorption by amine solutions: initial concentration of amine, inlet mole fraction of $CO_2$, and temperature were a) 0.2 M, 0.15, 25 °C; b) 0.1 M, 0.15, 25 °C; c) 0.2 M, 0.10, 25 °C; d) 0.2 M, 0.15, 40 °C, respectively.

620, 790, and 825 s for MEA, 2PE, PZ, and HPZ, respectively, and equilibrium was observed after 1650, 1830, 2050, and 2340 s for 2PE, PZ, HPZ, and MEA, respectively. When the amine concentration was reduced to half, the breakthrough time was approximately two times faster. The breakthrough curves in Figure 2c were obtained by reducing the initial mole fraction of $CO_2$ to 0.10 at 0.2 M amine concentration. When the gas mixture with a lower mole fraction of $CO_2$ was delivered to the column, the breakthrough time increased (1150, 1695, 1915, and 2670 s for MEA, 2PE, PZ, and HPZ, respectively) compared to the case of 0.15 of $CO_2$ mole fraction. The effect of temperature was investigated by increasing the temperature of the heating jacket from 25 to 40 °C while keeping the other parameters constant. The breakthrough times were obtained at 795, 1260, 1350, and 1685 s for MEA, PZ, 2PE, and HPZ, respectively. The breakthrough at 25 °C for MEA showed different behavior in comparison with the other amines. As shown in Figure 2a, the mole fraction of $CO_2$ in the breakthrough curve of MEA solution at 25 °C increased rapidly starting from the breakthrough time up to a certain time followed by a slow increase in the mole fraction until the equilibrium condition was reached. For the experiments done with MEA at 40 °C, the equilibrium condition was obtained at a longer time range and the breakthrough time appeared earlier compared to other amines. Generally, the breakthrough time was obtained in shorter time ranges for MEA than other amines. In all experiments performed at 25 °C, the breakthrough time increased in the order of MEA, 2PE, PZ, and HPZ (MEA the fastest, HPZ the slowest). In the experiments carried out at 40 °C, the breakthrough time of PZ was ahead of 2PE, and the breakthrough times increased in the order of MEA, PZ, 2PE, and HPZ.

The rate of $CO_2$ absorption for all experiments was calculated using equation (5) and plotted against the time, as shown in Figure 3. In all the curves shown, the rate of $CO_2$ absorption was constant for a certain period of time since the mole fraction of $CO_2$ at the outlet was zero during that period. After that period, the rate of $CO_2$ absorption was observed to decrease. Zwitterion mechanism which was first proposed by Caplow [27] and reintroduced by Danckwert [28] was widely used to interpret the kinetic data of $CO_2$ absorption into aqueous amine solutions. This mechanism consists of two main reactive steps. First, the nucleophilic nitrogen atom in the amine provides its electron pair to form a chemical bond with the electrophilic carbon atom of $CO_2$. As a result, an unstable compound called zwitterion is produced. Then, the formed zwitterion reacts with any base compound in the solution such as $OH^-$ and amine molecules (also $H_2O$) to form carbamate. Using this mechanism, the rate of the $CO_2$ absorption reactions is derived as a function of concentrations of amine,

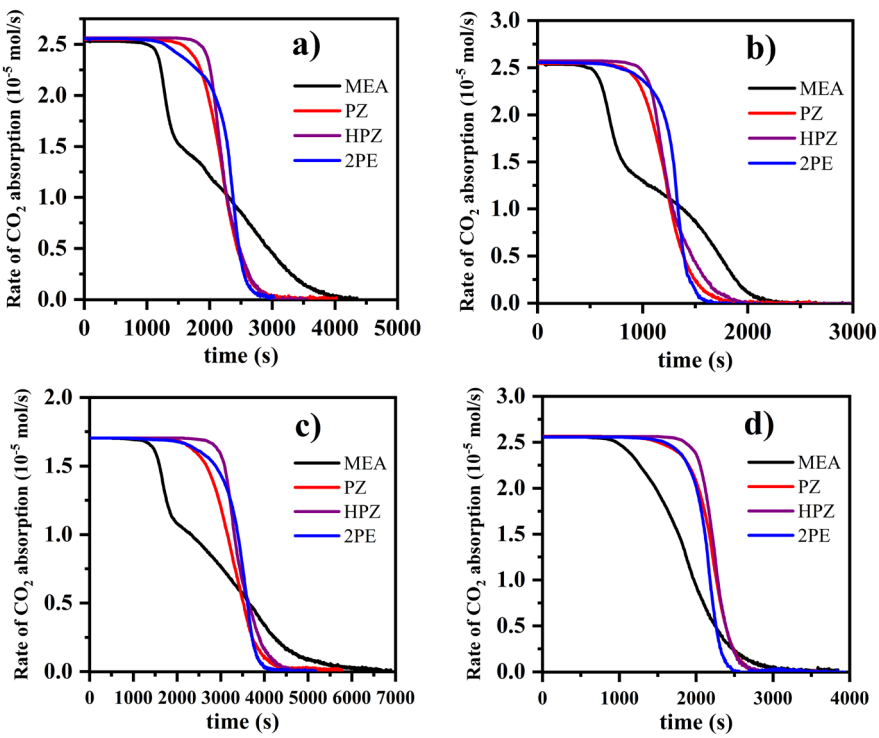


**Figure 3.** The rate of $CO_2$ absorption into amine solutions: initial concentration of amine, inlet mole fraction of $CO_2$, and temperature were a) 0.2 M, 0.15, 25 °C; b) 0.1 M, 0.15, 25 °C; c) 0.2 M, 0.10, 25 °C; d) 0.2 M, 0.15, 40 °C, respectively.

OH–, $H_2O$, and $CO_2$. According to the zwitterion mechanism, the rate of $CO_2$ absorption is proportional to the amine concentration [27–29]. As the amine becomes depleted due to the reaction with $CO_2$, the rate of $CO_2$ absorption decreases and finally reaches the thermodynamic equilibrium state at which the rate of $CO_2$ absorption becomes zero.

The cumulative amount of absorbed $CO_2$ was obtained by integration of absorption rate data versus time. Subsequently, the cumulative amount of absorbed $CO_2$ was divided by the initial number of moles of amine in the system to obtain the $CO_2$ loading of different amines. $CO_2$ loading of HPZ, 2PE, PZ, and MEA at different process conditions is presented in Figure 4. According to this figure, in the absorption runs with inlet $CO_2$ mole fraction of 0.15, HPZ showed the highest $CO_2$ loading with 1.32 and 1.18 mol $CO_2$/mol amine at 25 °C in both cases of 0.1 and 0.2 M of initial concentration of amines, respectively. $CO_2$ loading in any $CO_2$-$H_2O$-amine system depends on the concentration of amine, temperature, and partial pressure of $CO_2$. Even at a constant temperature at which the equilibrium constants of reactions are fixed, the equilibrium concentrations may change by changing the initial amounts of amine and $CO_2$ partial pressure in the system [18, 30]. Here, as the initial concentration of amine decreased, the $CO_2$ loading increased since a change in the initial concentration of the amine leads to the changes in the equilibrium concentrations of compounds in the vapor-liquid equilibrium system of $CO_2$-$H_2O$-amine [18,19]. The effect of inlet mole fraction of $CO_2$ and absorption temperature were also investigated. When the inlet mole fraction of $CO_2$ was reduced from 0.15 to 0.10, the $CO_2$ loading remained approximately constant for HPZ, PZ, and 2PE, but decreased for MEA. Increasing the temperature from 25 to 40 °C at constant amine concentration (0.2 M) and inlet mole fraction of $CO_2$ (0.15) resulted in a decrease in $CO_2$ loading of MEA, 2PE, PZ, and HPZ aqueous solutions from 1.06 to 0.95, 1.14 to 1.08, 1.13 to 1.12, and 1.18 to 1.15, respectively. In conclusion, as the inlet mole fraction of $CO_2$ increased and the initial concentration of amine and temperature decreased, the $CO_2$ loading increased. The obtained results were compared to the literature. Jou et al. [31] reported that the solubility of $CO_2$ in an MEA/$H_2O$ solution decreases by increasing the temperature and decreasing the $CO_2$ partial pressure. They reported a solubility of about 0.6 mol $CO_2$/mol amine at 25 °C, $CO_2$ partial pressure of 11.8 kPa, and 30 mass percent of MEA (5 mol/L). However, the concentrations used in our study (0.1 and 0.2 mol/L) were much lower than 5 mol/L resulting in a higher $CO_2$ loading which was in line with a trend that can be seen from the screening work conducted by Aronu et al. [30]. A similar result can be seen from another study, performed by Kim et al., which compared the $CO_2$ absorption characteristics of aqueous solutions of diamines. They reported a $CO_2$ loading of 0.775 and 0.839 mol $CO_2$/mol amine for 30 mass percent of PZ and HPZ solutions (5 mol/L) at 40 °C and $CO_2$ mole fraction of 0.3 in the inlet simulated gas stream. Here, they showed that increasing the temperature led to a decrease in the $CO_2$ loading. The $CO_2$ loading for lower amine concentrations was not reported [32]. Derks et al. reported that the $CO_2$ loading into the aqueous solution of piperazine decreased with an increase in temperature and amine concentration. For example, they observed that the $CO_2$ loading decreased from 1.02 to 0.98 mol $CO_2$/mol amine when the temperature increased from 25 to 40 °C for an aqueous solution with amin concentration of 0.2 mol/L and $CO_2$ partial pressure of approximately 10 kPa [33].

MEA and HPZ, the amines with the lowest and highest $CO_2$ loading as shown in Figure 4, were chosen to be studied in a wide range of initial concentrations of amine ranging from 0.02 up to 1 M. To that end, the temperature of amine

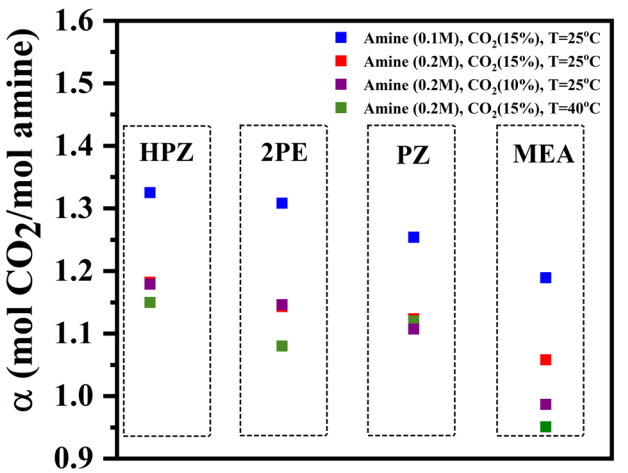


**Figure 4.** $CO_2$ loading of HPZ, 2PE, PZ, and MEA amines (inlet mixed gas flow rate has been kept constant at 250 mL/min for all experiments).

solutions, the total volumetric flow rate of the inlet gas mixture and the inlet mole fraction of $CO_2$ were kept constant in all experiments at 25 °C, 250 mL/min and 0.15, respectively. According to the breakthrough curves shown in Figure 5, breakthrough times with respect to the initial amine concentrations of 0.02, 0.1, 0.2, and 1 M, were found to be 105, 500, 1000, and 4500 s for MEA and 240, 825, 1700, and 9980 s for HPZ, respectively. At all concentrations analyzed, breakthrough with MEA was faster than HPZ. Also, as the amine concentration increased, the differences between the breakthrough times for MEA and HPZ increased.

$CO_2$ loading was calculated according to Equation 5 and the results are presented in Figure 6. As the initial concentration of MEA increased from 0.02 to 1 M, the $CO_2$ loading decreased from 2.25 to 0.72 mol $CO_2$/mol amine. The results were similar to the literature. Aronu et al. reported that at an MEA concentration of 1 mol/L, the $CO_2$ loading was obtained as 0.66 mol $CO_2$/mol amine which was very close to the value obtained in our study (0.72 mol $CO_2$/mol amine). Also, they showed that by further increasing MEA concentration from 1 to 5 mol/L, the $CO_2$ loading decreased from 0.66 to 0.53 mol $CO_2$/mole MEA. The curve of $CO_2$ loading versus the amine concentration showed that using the amine concentrations lower than 1 mol/L led to a further increase of the $CO_2$ loading, in line with results reported in our study. In addition, they showed that decreasing the $CO_2$ partial pressure from 15 to 9.5 kPa led to a decrease in the $CO_2$ loading for different

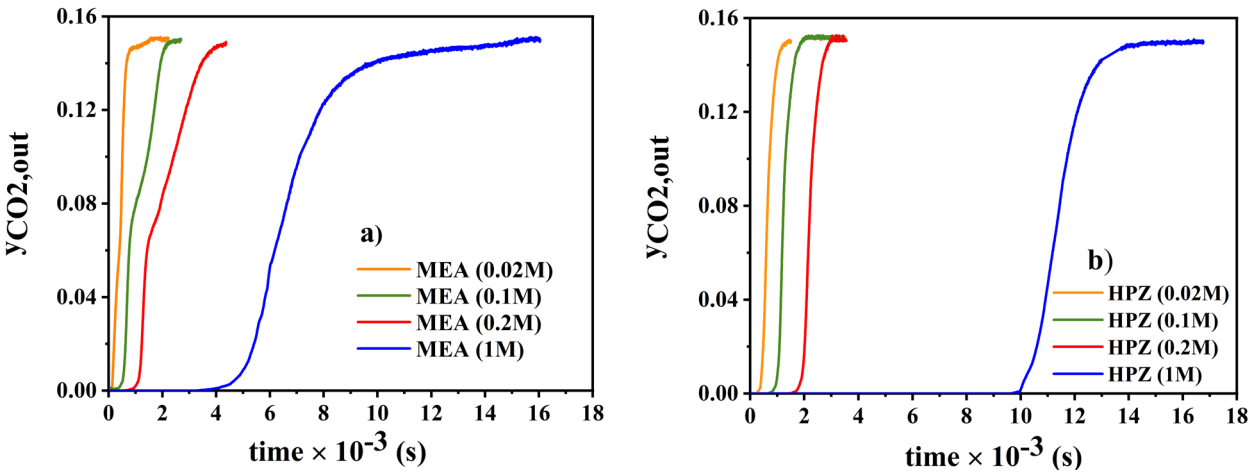


**Figure 5.** Effect of initial concentration of MEA and HPZ amines: a) MEA, b) HPZ (inlet mole fraction of $CO_2$: 0.15, temperature: 25 ° C, the volumetric flow rate of the inlet gas mixture: 250 mL/min).

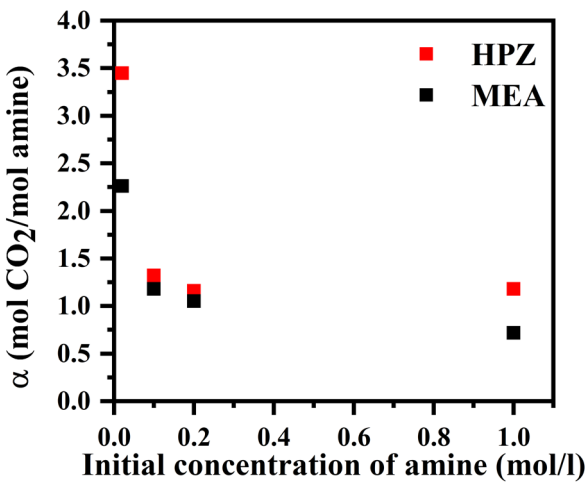


**Figure 6.** $CO_2$ loading versus initial concentration of amines in HPZ and MEA solutions (inlet mole fraction of $CO_2$: 0.15, temperature: 25 °C, volumetric flow rate of the inlet gas mixture: 250 mL/min).

MEA concentrations [18]. In experiments with HPZ, as the amine concentration increased from 0.02 M to 0.2 M, the $CO_2$ loading decreased from 3.45 to 1.15 mol $CO_2$/mol amine and remained almost constant by a further increase in the initial concentration of HPZ from 0.2 to 1 M.

### 3.2. pH of the solution

According to the zwitterion mechanism [34, 35], the rate of $CO_2$ absorption is affected by the concentration of the hydroxyl ion as well as the amine and $CO_2$ concentration. In this mechanism, as the concentration of the hydroxyl ion decreases, the rate of $CO_2$ absorption also decreases. For this purpose, the pH values of the amine solutions at the beginning and the $CO_2$ saturation point were measured in the experiments performed at 25 °C, 0.2 M of initial amine concentration, and 0.15 of inlet $CO_2$ mole fraction. The results are presented in Figure 7. Amine solutions were initially basic with pH values above 11. Table 1 shows the reactions which are expected to take place in the $CO_2$-amine-water system during the absorption/desorption [31, 34, 36, 37]. pH values above 11 of amine solutions before feeding $CO_2$ was due to protonation of amine shown by reaction R4 in Table 1, consuming hydronium ions. The pH values decreased after the solutions were fed with $CO_2$. According to reactions in Table 1, as the solution was fed with $CO_2$, the reaction R2 goes in the forward direction producing bicarbonate ions and hydronium ions. The produced bicarbonate ions are consumed by amine in the forward reaction R5. This decreases the bicarbonate ion concentration forcing reaction R2 to proceed in the forward direction producing more bicarbonate ions as well as hydronium ions. A portion of hydronium ions is also produced by forward reaction of R3. As a result, the increase in hydronium ion concentration, as well as a decrease in hydroxyl

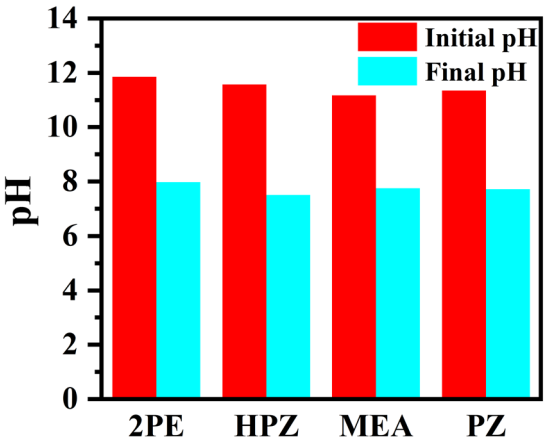


**Figure 7.** pH values of amine solutions at the beginning and at the end of $CO_2$ absorption (initial amine concentration 0.2 M, input $CO_2$ concentration 0.15, gas mixture flow rate 250 mL/min, temperature 25 °C).

**Table 1.** Reactions occurring in the liquid phase during absorption of $CO_2$ by an amine solution [30, 32–34].

| Reaction | Reaction number |
|---|---|
| $2H_2O \underset{k-1}{\overset{k1}{\rightleftharpoons}} H_3O^+ + OH^-$ | (R1) |
| $CO_2 + 2H_2O \underset{k_{-2}}{\overset{k_2}{\rightleftharpoons}} HCO_3^- + H_3O^+$ | (R2) |
| $HCO_3^- + H_2O \underset{k_{-3}}{\overset{k_3}{\rightleftharpoons}} CO_3^{2-} + H_3O^+$ | (R3) |
| $R_1R_2NH + H_3O^+ \underset{k_{-4}}{\overset{k_4}{\rightleftharpoons}} R_1R_2NH_2^+ + H_2O$ | (R4) |
| $R_1R_2NH + HCO_3^- \underset{k_{-5}}{\overset{k_5}{\rightleftharpoons}} R_1R_2NCOO^- + H_2O$ | (R5) |
| $R_1R_2NCOO^- + H_3O^+ \underset{k_{-6}}{\overset{k_6}{\rightleftharpoons}} R_1R_2NH^+COO^- + H_2O$ | (R6) |

ion, causes the pH value of the solution to decrease. Initial and posttreatment pH values decreased from 11.86 to 7.98, 11.57 to 7.51, 11.17 to 7.76, and from 11.35 to 7.72 for 2PE, HPZ, MEA, and PZ, respectively. Since the solution came to thermodynamic equilibrium after the treatment, the solution was not completely neutralized since the unreacted amines stay in the solution even if their concentration was small.

### 3.3. Effect of copper ions

In electrochemical amine regeneration systems, the amine-$CO_2$ complex is pumped to the anode of an electrochemical cell where the metal ions (e.g., Cu(II)) are dissolved by the potential applied to the anode. These metal ions compete with $CO_2$ to form a complex with the amine, allowing the release of $CO_2$. The obtained metal(II)-amine complexes are pumped to the cathode in the electrochemical cell to reduce the metal ion and regenerate the amine (reduced metal ions accumulate in the solid metal form on the cathode). Copper is the most preferred metal to be used in these electrochemical cells [24]. The presence of copper ions in the regenerated amine solution affects the $CO_2$ loading of the solution. For this reason, the $CO_2$ loading of amine solutions with different copper ion concentrations was measured. Copper(II) nitrate was added to the solutions to prepare the certain concentrations of copper ions in the solutions. Precipitation was observed for 2PE and PZ amines as copper ions were introduced into the solution. For this reason, only aqueous solutions containing MEA and HPZ were subjected to $CO_2$ absorption in the presence of copper ions. MEA and HPZ solutions with copper ions in a concentration range of 0.02–0.1 M were prepared. The initial concentration of amine, the inlet mole fraction of $CO_2$, inlet gas mixture volumetric flow rate, and temperature of the solution were kept constant at 0.2 M, 0.15, 250 mL/min, and 40 °C, respectively. According to Figures 8a and b, as the copper concentration increased in MEA and HPZ solutions, the breakthrough time decreased.

Figure 9 shows the $CO_2$ loading of each case calculated by integration of the absorption rate of $CO_2$ versus time, as explained in section 2.3. It was found that as the concentration of copper (II) ions increased, $CO_2$ loading for both HPZ and MEA decreased significantly from 1.15 (0 M copper) to 0.33 mol $CO_2$/mol HPZ (0.1 M copper), and from 0.95 (0 M copper) to 0.59 mol $CO_2$/mol MEA (0.05 M copper), respectively. Reactions R7, R8, R9, and R10 shown in Table 2 indicate that copper ions react with one, two, three, or four amines, respectively, and form different types of copper (II)-amine complexes [26]. Only a very small fraction of the copper(II)-amine complexes can form free amines as a result of the reverse reaction. Thus, the concentration of free amines in this system is smaller compared to that of copper-free amine solutions since most of the copper(II)-amine complexes are not regenerated as free amine due to higher equilibrium constants of copper (II)-amine complex formation reactions [26, 38]. As a result, $CO_2$ loading in systems containing copper (II) ions decreases. According to Figure 9, the decreases in $CO_2$ loading due to the presence of copper ions were observed for both MEA and HPZ. Especially the large change in $CO_2$ loading in case of HPZ is promising for electrochemical amine regeneration.

## 4. Conclusion

The process of $CO_2$ capture by amine-based chemical absorption routes has high $CO_2$ removal efficiency and is easy to scale up. The physical and chemical properties of amine-$H_2O$-$CO_2$ systems affect the $CO_2$ removal efficiency. Among them, viscosity, density, solubility of $CO_2$, type of amine, rate of reaction, rate of mass transfer, and heat of regeneration are the

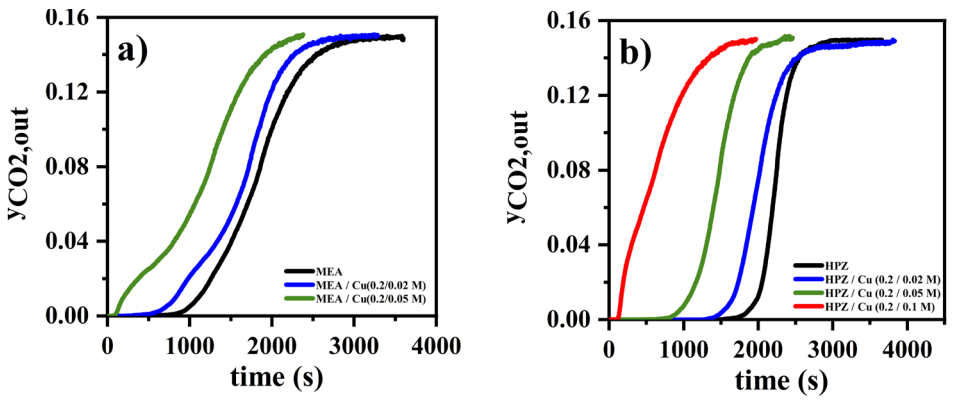


**Figure 8.** Copper ion effect (0.2 M of initial concentration of amine, 0.15 of inlet mole fraction of $CO_2$, 40 °C of temperature) (No data for 0.2 M MEA solution at 0.1 M Cu(II) concentration was obtained since precipitation was observed).

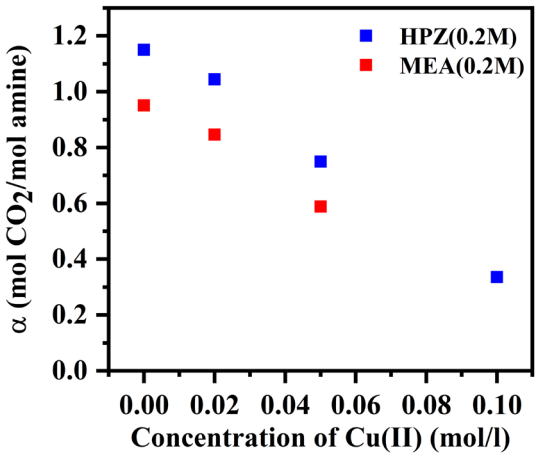


**Figure 9.** Change of $CO_2$ loading with Cu(II) concentration for HPZ and MEA solutions. (No data for 0.2 M MEA solution at 0.1 M Cu(II) concentration was obtained since precipitation was observed).

**Table 2.** Reactions of Cu with amine in Cu–amine–$CO_2$–$H_2O$ system [26].

| Reaction | Reaction number |
|---|---|
| $Cu^{2+} + R_1R_2NH \rightleftarrows Cu(R_1R_2NH)^{2+}$ | (R7) |
| $Cu^{2+} + 2R_1R_2NH \rightleftarrows Cu(R_1R_2NH)_2^{2+}$ | (R8) |
| $Cu^{2+} + 3R_1R_2NH \rightleftarrows Cu(R_1R_2NH)_3^{2+}$ | (R9) |
| $Cu^{2+} + 4R_1R_2NH \rightleftarrows Cu(R_1R_2NH)_4^{2+}$ | (R10) |

important factors affecting the $CO_2$ removal efficiency. In this study, the effect of type of amine on $CO_2$ loading at different amine concentrations, inlet mole fractions of $CO_2$, and temperatures was investigated. Aqueous solutions of four different amines including MEA, 2PE, PZ, and HPZ were used as the absorbent for chemical absorption of $CO_2$ using a nonstirred bubble column. $CO_2$ loading of MEA, 2PE, PZ, and HPZ aqueous solutions at 25 °C, 0.2 M of initial concentration of amine, and 0.15 of inlet mole fraction of $CO_2$ was 1.06, 1.14, 1.13, and 1.18 mol $CO_2$/mol amine, respectively. Thus, the highest $CO_2$ loading was observed for HPZ among the studied amines. By decreasing the inlet mole fraction of $CO_2$ from 0.15 to 0.10, the $CO_2$ loading slightly decreased. As the initial concentration of amine decreased to 0.1 M, the $CO_2$ loading increased to 1.19, 1.30, 1.25, 1.32 mol $CO_2$/mol amine for MEA, 2PE, PZ, and HPZ, respectively. Also, increasing the temperature up to 40 °C decreased the $CO_2$ loading to 0.95, 1.08, 1.12, 1.15 mol $CO_2$/mol amine for MEA, 2PE, PZ, and HPZ, respectively. The $CO_2$ removal efficiency of the interested amine solutions in presence of copper ions was also investigated. The results demonstrated that the addition of copper ions to the fresh amine solution leads to a decrease in the $CO_2$ loading of MEA and HPZ aqueous solutions. Increasing the concentration of copper ions from 0 to 0.05 M resulted in a decrease in $CO_2$ loading at 40 °C, from 1.15 to 0.75 and 0.95 to 0.59 mol $CO_2$/mol amine for HPZ and MEA, respectively. Further increase in the concentration of copper ions to 0.1 M led to precipitation in MEA solution and a further decrease in $CO_2$ loading to 0.34 mol $CO_2$/mol amine for HPZ solution. However, in the case of PZ and 2PE amines, adding copper ions led to precipitation even at low copper ion concentrations.

**Acknowledgment**
Financial support of Turkish Scientific and Technological Research Council (TÜBİTAK) under project no. 218M850 is acknowledged.

Nomenclature

| | |
|---|---|
| $N_i$ | number of moles of species *i,* mol |
| $F_i$ | molar flow rate of species *i*, mol/s |
| $r_{i,\,(absorption)}$ | rate of absorption of species *i*, mol/s |
| $t$ | time, s |
| $C_i$ | concentration of species *i*, mol/m$^3$ |
| $V_g$ | volume of gas phase, m$^3$ |
| $y_i$ | mole fraction of species *i*, mol/mol |
| $P$ | pressure, Pa |
| $T$ | temperature, K |
| $R$ | gas constant, J/(mol.K) |
| $\alpha_{CO_2}$ | $CO_2$ loading, mol $CO_2$/mol amine |

## References


1. Ochedi FO, Yu J, Yu H, Liu Y, Hussain A. Carbon dioxide capture using liquid absorption methods: a review. Environmental Chemistry Letters 2020; 19 (1): 77-109. doi: 10.1007/s10311-020-01093-8

2. Aghaie M, Rezaei N, Zendehboudi S. A systematic review on $CO_2$ capture with ionic liquids: Current status and future prospects. Renewable and Sustainable Energy Reviews 2018; 96: 502-525. doi: 10.1016/j.rser.2018.07.004

3. Mikkelsen M, Jørgensen M, Krebs FC. The teraton challenge. A review of fixation and transformation of carbon dioxide. Energy & Environmental Science 2010; 3 (1): 43-81. doi: 10.1039/b912904a

4. Cannone SF, Lanzini A, Santarelli M. A Review on CO2 Capture Technologies with Focus on CO2-Enhanced Methane Recovery from Hydrates. Energies 2021; 14 (2). doi: 10.3390/en14020387

5. Wang Y, Zhao L, Otto A, Robinius M, Stolten D. A Review of Post-combustion $CO_2$ Capture Technologies from Coal-fired Power Plants. Energy Procedia 2017; 114: 650-665. doi: 10.1016/j.egypro.2017.03.1209

6. Milner PJ, Siegelman RL, Forse AC, Gonzalez MI, Runcevski T et al. A Diaminopropane-Appended Metal-Organic Framework Enabling Efficient $CO_2$ Capture from Coal Flue Gas via a Mixed Adsorption Mechanism. Journal of the American Chemical Society 2017; 139 (38): 13541-13553. doi: 10.1021/jacs.7b07612

7. Conway W, Fernandes D, Beyad Y, Burns R, Lawrance G et al. Reactions of $CO_2$ with aqueous piperazine solutions: formation and decomposition of mono- and dicarbamic acids/carbamates of piperazine at 25.0 degrees C. J Phys Chem A 2013; 117 (5): 806-813. doi: 10.1021/jp310560b

8. Sreedhar I, Vaidhiswaran R, Kamani BM, Venugopal A. Process and engineering trends in membrane based carbon capture. Renewable and Sustainable Energy Reviews 2017; 68: 659-684. doi: 10.1016/j.rser.2016.10.025

9. Song C, Liu Q, Deng S, Li H, Kitamura Y. Cryogenic-based $CO_2$ capture technologies: State-of-the-art developments and current challenges. Renewable and Sustainable Energy Reviews 2019; 101: 265-278. doi: 10.1016/j.rser.2018.11.018

10. Kronberger B, Johansson E, Löffler G, Mattisson T, Lyngfelt A et al. A Two-Compartment Fluidized Bed Reactor for $CO_2$ Capture by Chemical-Looping Combustion. Chemical Engineering & Technology 2004; 27 (12): 1318-1326. doi: 10.1002/ceat.200402137

11. Liu S, Gao H, He C, Liang Z. Experimental evaluation of highly efficient primary and secondary amines with lower energy by a novel method for post-combustion $CO_2$ capture. Applied Energy 2019; 233-234: 443-452. doi: 10.1016/j.apenergy.2018.10.031

12. Chalmers H, Gibbins J. Initial evaluation of the impact of post-combustion capture of carbon dioxide on supercritical pulverised coal power plant part load performance. Fuel 2007; 86 (14): 2109-2123. doi: 10.1016/j.fuel.2007.01.028

13. Abu-Zahra MRM, Schneiders LHJ, Niederer JPM, Feron PHM, Versteeg GF. $CO_2$ capture from power plants. International Journal of Greenhouse Gas Control 2007; 1 (1): 37-46. doi: 10.1016/s1750-5836(06)00007-7

14. Didas SA, Kulkarni AR, Sholl DS, Jones CW. Role of amine structure on carbon dioxide adsorption from ultradilute gas streams such as ambient air. ChemSusChem 2012; 5 (10): 2058-2064. doi: 10.1002/cssc.201200196

15. Seo DJ, Hong WH. Effect of Piperazine on the Kinetics of Carbon Dioxide with Aqueous Solutions of 2-Amino-2-methyl-1-propanol. Industrial & Engineering Chemistry Research 2000; 39 (6): 2062-2067. doi: 10.1021/ie990846f

16. Dugas R, Rochelle G. Absorption and desorption rates of carbon dioxide with monoethanolamine and piperazine. Energy Procedia 2009; 1 (1): 1163-1169. doi: 10.1016/j.egypro.2009.01.153

17. Moioli S, Pellegrini LA. Modeling the methyldiethanolamine-piperazine scrubbing system for $CO_2$ removal: Thermodynamic analysis. Frontiers of Chemical Science and Engineering 2016; 10 (1): 162-175. doi: 10.1007/s11705-016-1555-5

18. Aronu UE, Gondal S, Hessen ET, Haug-Warberg T, Hartono A et al. Solubility of $CO_2$ in 15, 30, 45 and 60 mass% MEA from 40 to 120°C and model representation using the extended UNIQUAC framework. Chemical Engineering Science 2011; 66 (24): 6393-6406. doi: 10.1016/j.ces.2011.08.042

19. Thee H, Suryaputradinata YA, Mumford KA, Smith KH, Silva Gd et al. A kinetic and process modeling study of $CO_2$ capture with MEA-promoted potassium carbonate solutions. Chemical Engineering Journal 2012; 210: 271-279. doi: 10.1016/j.cej.2012.08.092

20. Tong D, Trusler JPM, Maitland GC, Gibbins J, Fennell PS. Solubility of carbon dioxide in aqueous solution of monoethanolamine or 2-amino-2-methyl-1-propanol: Experimental measurements and modelling. International Journal of Greenhouse Gas Control 2012; 6: 37-47. doi: 10.1016/j.ijggc.2011.11.005

21. Ling H, Liu S, Wang T, Gao H, Liang Z. Characterization and Correlations of $CO_2$ Absorption Performance into Aqueous Amine Blended Solution of Monoethanolamine (MEA) and N,N-Dimethylethanolamine (DMEA) in a Packed Column. Energy & Fuels 2019; 33 (8): 7614-7625. doi: 10.1021/acs.energyfuels.9b01764

22. Duan L, Zhao M, Yang Y. Integration and optimization study on the coal-fired power plant with $CO_2$ capture using MEA. Energy 2012; 45 (1): 107-116. doi: 10.1016/j.energy.2011.12.014

23. Rheinhardt JH, Singh P, Tarakeshwar P, Buttry DA. Electrochemical Capture and Release of Carbon Dioxide. ACS Energy Letters 2017; 2 (2): 454-461. doi: 10.1021/acsenergylett.6b00608

24. Stern MC, Hatton TA. Bench-scale demonstration of $CO_2$ capture with electrochemically-mediated amine regeneration. RSC Advances 2014; 4 (12). doi: 10.1039/c3ra46774k

25. Shaw RA, Hatton TA. Electrochemical $CO_2$ capture thermodynamics. International Journal of Greenhouse Gas Control 2020; 95. doi: 10.1016/j.ijggc.2019.102878

26. Cheng C-h, Li K, Yu H, Jiang K, Chen J et al. Amine-based post-combustion $CO_2$ capture mediated by metal ions: Advancement of $CO_2$ desorption using copper ions. Applied Energy 2018; 211: 1030-1038. doi: 10.1016/j.apenergy.2017.11.105

27. Caplow M. Kinetics of carbamate formation and breakdown. Journal of the American Chemical Society 1968; 90 (24): 6795-6803. doi: 10.1021/ja01026a041

28. Danckwerts PV. The reaction of $CO_2$ with ethanolamines. Chemical Engineering Science 1979; 34 (4): 443-446. doi: 10.1016/0009-2509(79)85087-3

29. Blauwhoff PMM, Versteeg GF, Van Swaaij WPM. A study on the reaction between $CO_2$ and alkanolamines in aqueous solutions. Chemical Engineering Science 1983; 38 (9): 1411-1429. doi: 10.1016/0009-2509(83)80077-3

30. Bernhardsen IM, Knuutila HK. A review of potential amine solvents for $CO_2$ absorption process: Absorption capacity, cyclic capacity and pKa. International Journal of Greenhouse Gas Control 2017; 61: 27-48. doi: 10.1016/j.ijggc.2017.03.021

31. Jou F-Y, Mather AE, Otto FD. The solubility of $CO_2$ in a 30 mass percent monoethanolamine solution. The Canadian Journal of Chemical Engineering 1995; 73 (1): 140-147. doi: 10.1002/cjce.5450730116

32. Kim YE, Yun SH, Choi JH, Nam SC, Park SY et al. Comparison of the $CO_2$ Absorption Characteristics of Aqueous Solutions of Diamines: Absorption Capacity, Specific Heat Capacity, and Heat of Absorption. Energy & Fuels 2015; 29 (4): 2582-2590. doi: 10.1021/ef500561a

33. Derks PWJ, Dijkstra HBS, Hogendoorn JA, Versteeg GF. Solubility of carbon dioxide in aqueous piperazine solutions. AIChE Journal 2005; 51 (8): 2311-2327. doi: 10.1002/aic.10442

34. Heydarifard M, Pashaei H, Ghaemi A, Nasiri M. Reactive absorption of $CO_2$ into Piperazine aqueous solution in a stirrer bubble column: Modeling and experimental. International Journal of Greenhouse Gas Control 2018; 79: 91-116. doi: 10.1016/j.ijggc.2018.09.017

35. Pashaei H, Ghaemi A, Nasiri M. Modeling and experimental study on the solubility and mass transfer of $CO_2$ into aqueous DEA solution using a stirrer bubble column. RSC Advances 2016; 6 (109): 108075-108092. doi: 10.1039/c6ra22589f

36. Deshmukh RD, Mather AE. A mathematical model for equilibrium solubility of hydrogen sulfide and carbon dioxide in aqueous alkanolamine solutions. Chemical Engineering Science 1981; 36 (2): 355-362. doi: 10.1016/0009-2509(81)85015-4

37. Benamor A, Aroua MK. Modeling of $CO_2$ solubility and carbamate concentration in DEA, MDEA and their mixtures using the Deshmukh–Mather model. Fluid Phase Equilibria 2005; 231 (2): 150-162. doi: 10.1016/j.fluid.2005.02.005

38. Zhang M, Liu Y, Zhu Y, Wu K, Lu H et al. Cu(II)-Assisted $CO_2$ Absorption and Desorption Performances of the MMEA–$H_2O$ System. Energy & Fuels 2021; 35 (11): 9509-9520. doi: 10.1021/acs.energyfuels.1c00633